Supplementary Information for

Multiple hydrogen bonding crosslinked graphene oxide films with improved stretchability and toughness

Mengling Yang[1], Chunyu Wang[1*], Wenbin Wang[1], Li Yang[1], Shaolei Qu[1], Zhaoming Zhang[1], and Xuzhou Yan[1*]

[1]School of Chemistry and Chemical Engineering, Frontiers Science Center for Transformative Molecules, Shanghai Jiao Tong University, Shanghai 200240, P. R. China.

[*]Corresponding authors. E-mails: rainywang@sjtu.edu.cn, xzyan@sjtu.edu.cn

1. Materials and general methods

All reagents were commercially available and used as supplied without further purification. Deuterated solvents were purchased from Cambridge Isotope Laboratory (Andover, MA). Compounds UPyMA was prepared according to the established methods[1–3]. For the reported compound, only ^{1}H NMR spectra was measured and compared with those in literatures to prove its structure.

Nuclear magnetic resonance (NMR) spectra were recorded with a Bruker Avance DMX 400 spectrophotometer with use of the deuterated solvent as the lock and the residual solvent or TMS as the internal reference. Gel permeation chromatography (GPC) analysis was performed using an HLC-8320 GPC (TOSOH, Japan) instrument using N, N-Dimethylformamide (DMF) as eluent with polymethyl methacrylate (PMMA) standards. Fourier transform infrared (FT-IR) spectroscopy was performed on a Thermoscientific Nicolet 6700 FT-IR spectrometer at room temperature in the range of 550~4000 cm^{-1}. The thermal stability analysis was conducted using a TA Instruments Q500 thermogravimetric analyzer (TGA) under the nitrogen. Each sample (~5 mg) was heated from ambient temperature to 500 °C with a heating rate of 20.0 °C/min. X-ray photoelectron spectroscopy (XPS) spectra were obtained using an X-ray photoelectron spectrometer (AXIS UltraDLD, Shimadzu) with a monochromatic Al-Kα X-ray source. Scanning electron microscope (SEM) images were observed applying a field emission SEM (Apreo 2S, FEI Company) at an acceleration voltage of 5 kV. X-ray diffraction (XRD) measurements was done by X-ray diffractometer (Aeris, Malvern Panalytical) using Cu-Kα radiation at a scanning speed of 2°/min. Then, the interlayer spacing (d) can be calculated according to Bragg's Law, $2d\sin\theta = n\lambda$, where θis half of 2θ at 002 peak in XRD curves, n (diffraction order) and λ (X-ray wavelength) equal to 1 and 0.154 nm, respectively. Atomic force microscopy (AFM, Multimode 8, Bruker) was utilized to measure the surface adhesion of GO films.

The mechanical tensile test was accomplished by means of a tensile tester (Instron 3343) with a 100 N sensor under air atmosphere and room temperature. Before testing, the samples were cropped to a length of 15 mm and a width of 3 mm. On top of that, paper frames with a rectangular hole were tailored, of which the hole could accommodate the sample in width. The sample strips were adhesively attached to the paper frames so that the samples would not be damaged when clamped via gauges. The gauge length was set to 5 mm and the legs of paper frames were cut when

loading samples was completed. Tensile stress–strain curves were acquired at a loading rate of 1 mm/min. Young's modulus was determined from the slope of the linear part of the stress–strain curves. Toughness was obtained from the area under the tensile stress−strain curve until the sample fractured. Energy dissipation was calculated by integrating the area encompassed by the cyclic tensile curves. Damping capacity was defined as the ratio of the dissipated energy (the area encompassed by the loading and unloading curves) to the loading energy (the area encompassed by the loading curve).

2. Synthesis of PUPy and PBMA

Synthesis of UPyMA

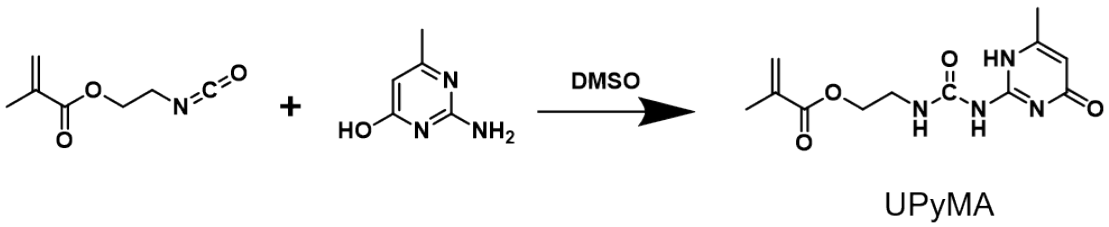

2-Amino-4-hydroxy-6-methylpyrimidine (2.00 g, 15.98 mmol) was added into 80 mL of DMSO and stirred for 10 min at 150 °C. Then the solution was cooled to room temperature and 2-isocyanatoethyl methacrylate (2.70 g, 17.40 mmol) was added into the flask. The mixture was kept stirring for 12 h at room temperature. The white precipitates were collected by filtration, washed with *n*-hexane. Finally, the precipitates were dried under vacuum at 30 °C for 4 h to afford UPyMA as a white powder (2.71 g, 60%). The ^{1}H NMR spectrum of UPyMA is shown in Figure S1. ^{1}H NMR ($CDCl_3$, room temperature, 400 MHz) δ (ppm): 12.97 (s, 1H), 11.95 (s, 1H), 10.50 (s, 1H), 6.21–6.16 (m, 1H), 5.79 (s, 1H), 5.55–5.54 (m, 1H), 4.27 (t, J = 5.7 Hz, 2H), 3.60–3.56 (m, 2H), 2.23 (d, J = 1.0 Hz, 3H), 1.93 (t, J = 1.3 Hz, 3H).

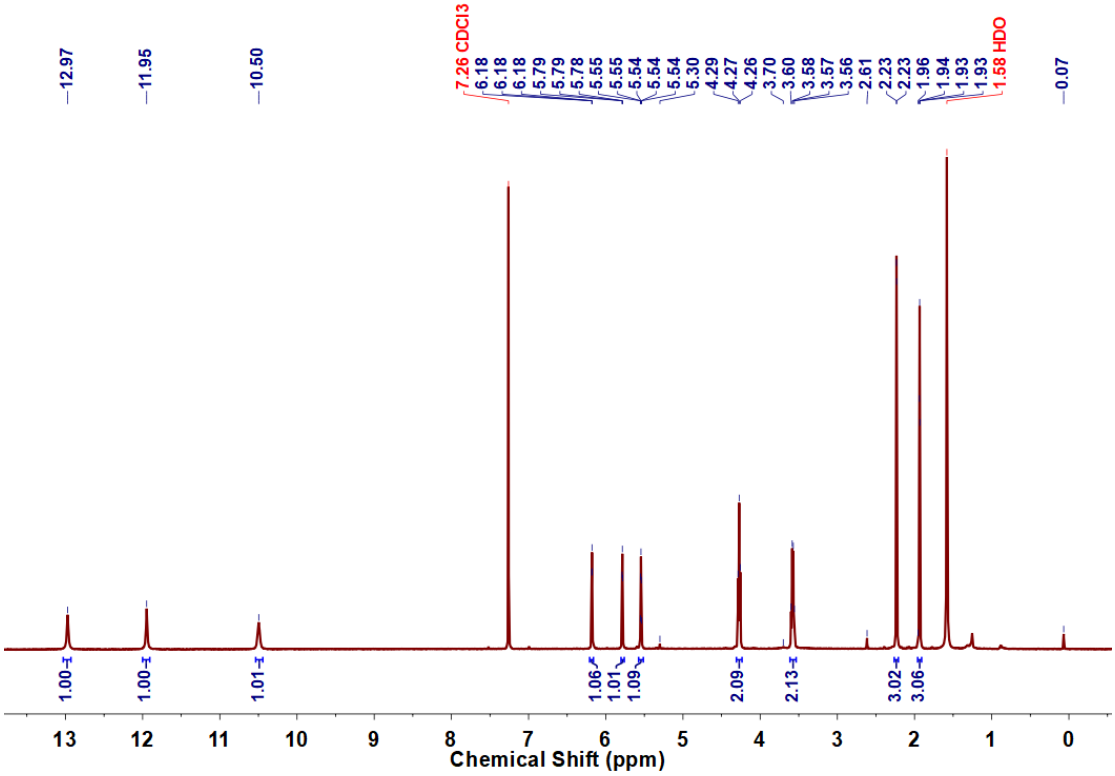

Figure S1. ^{1}H NMR spectrum ($CDCl_3$, room temperature, 400 MHz) of UPyMA.

Synthesis of PUPy

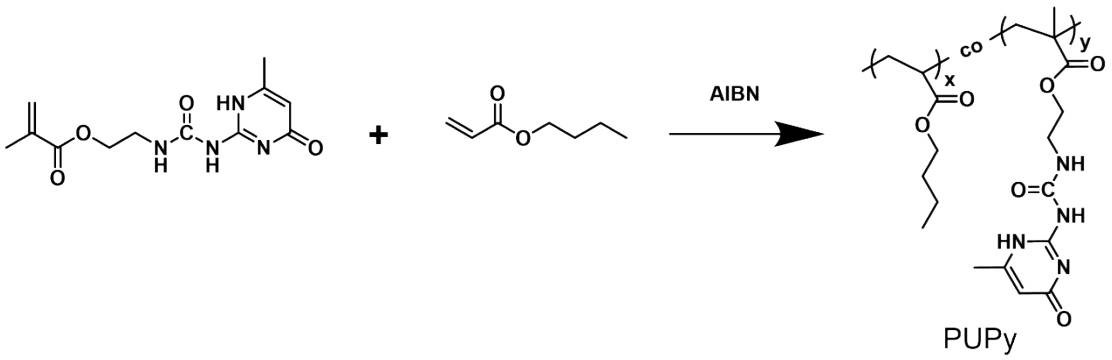

UPyMA (300 mg, 1.07 mmol), butyl acrylate (BA, 1.37 g, 10.7 mmol), azobis(isobutyronitrile) as thermal initiator (AIBN, 19 mg, 0.12 mmol) and DMF were added to a vial, and stirring at room temperature until all monomers were completely dissolved. Then, was degassed three times via the freeze-thaw technique. The polymerization reaction was carried out at 80 °C under nitrogen atmosphere for 24h. After cooling at room temperature, the reaction mixture was precipitated in ice methanol, then filtered, and dried at 60 °C for 24 h to obtain PUPy as a colorless gelatinous solid. The ^{1}H NMR spectrum of PUPy is shown in Figure S2.

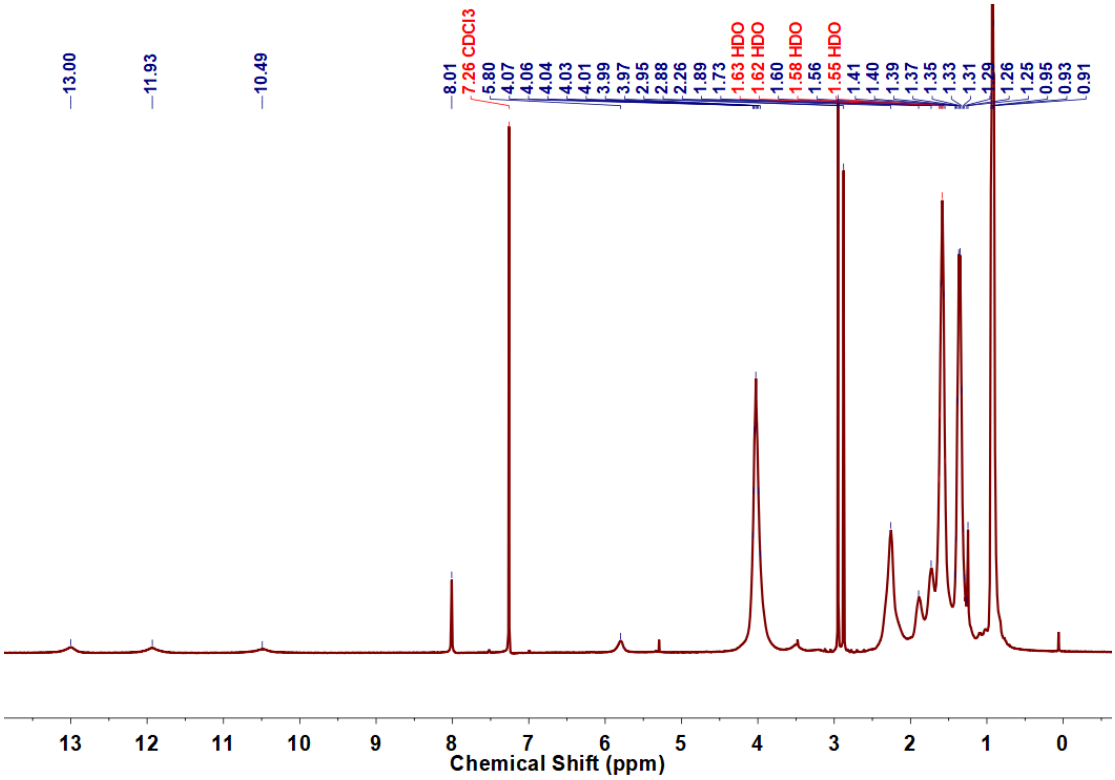

Figure S2. ^{1}H NMR spectrum ($CDCl_3$, room temperature, 400 MHz) of PUPy.

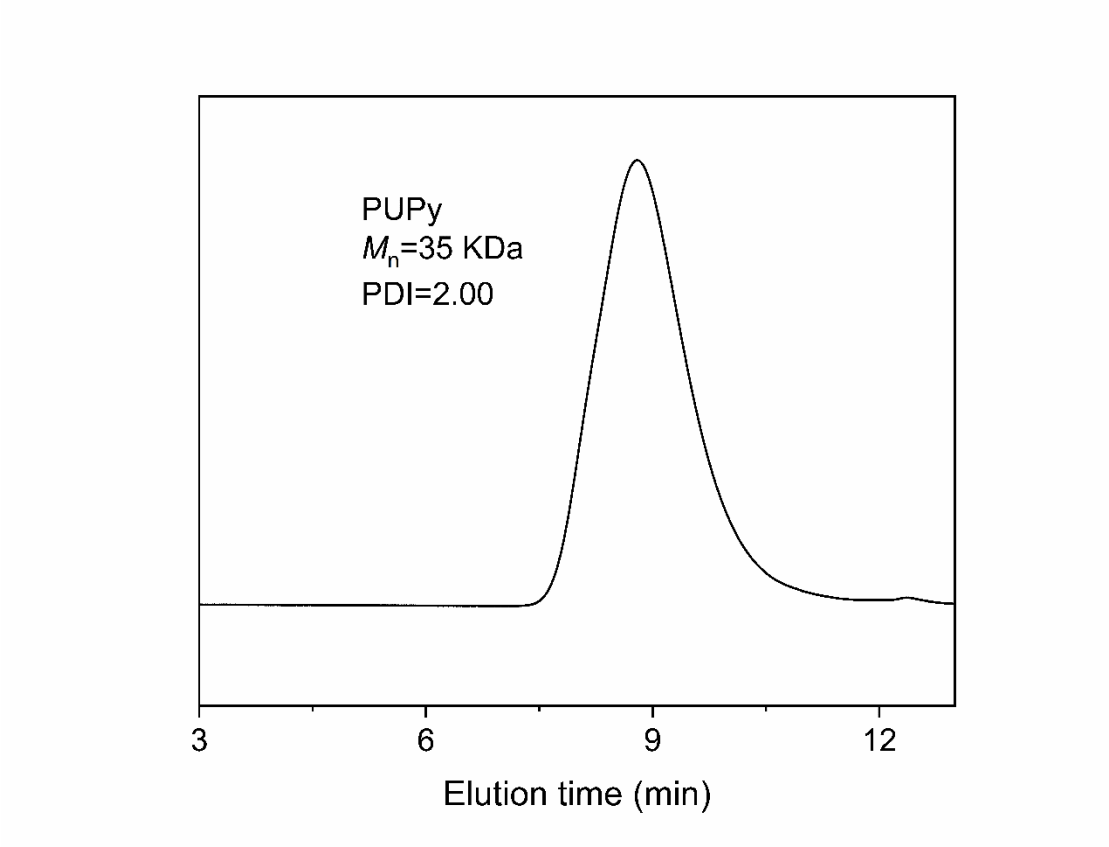

Figure S3. GPC elution curve of the PUPy with DMF as the eluent and PMMA as the standard.

Synthesis of PBMA

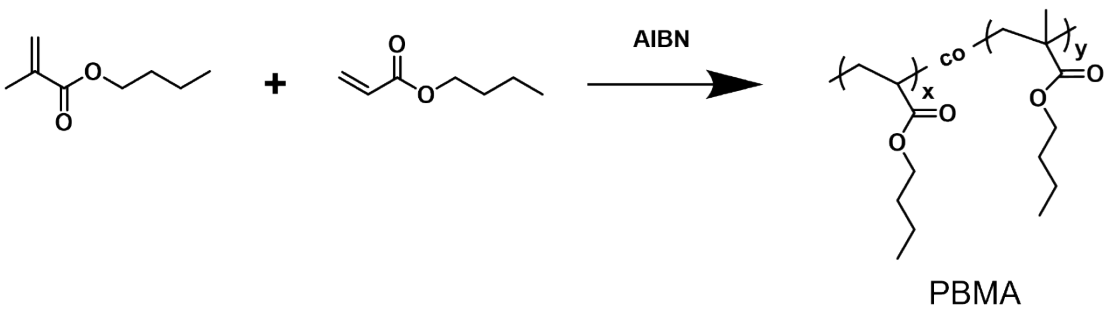

Butyl methacrylate (BMA, 152 mg, 1.07 mmol), butyl acrylate (BA, 1.37 g, 10.7 mmol), azobis(isobutyronitrile) as thermal initiator (AIBN, 19 mg, 0.12 mmol) and DMF were added to a vial, and stirring at room temperature until all monomers were completely dissolved. Then, the solution was degassed three times via the freeze-thaw technique. The polymerization reaction was carried out at 80 °C under nitrogen atmosphere for 24h. After cooling at room temperature, the reaction mixture was precipitated in ice methanol, then filtered, and dried at 60 °C for 24 h to obtain

PBMA as a colorless viscous liquid. The ^{1}H NMR spectrum of PBMA is shown in Figure S3. GPC elution curve of the PBMA is shown in Figure S4.

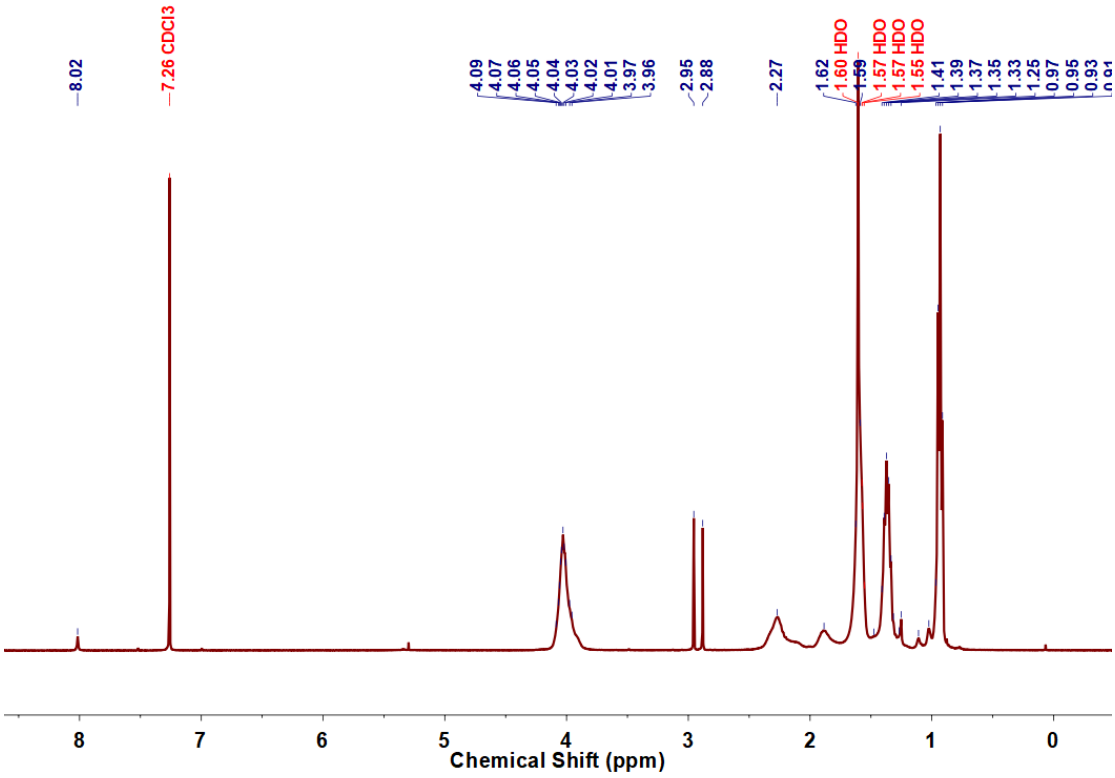

Figure S4. ^{1}H NMR spectrum ($CDCl_3$, room temperature, 400 MHz) of PBMA.

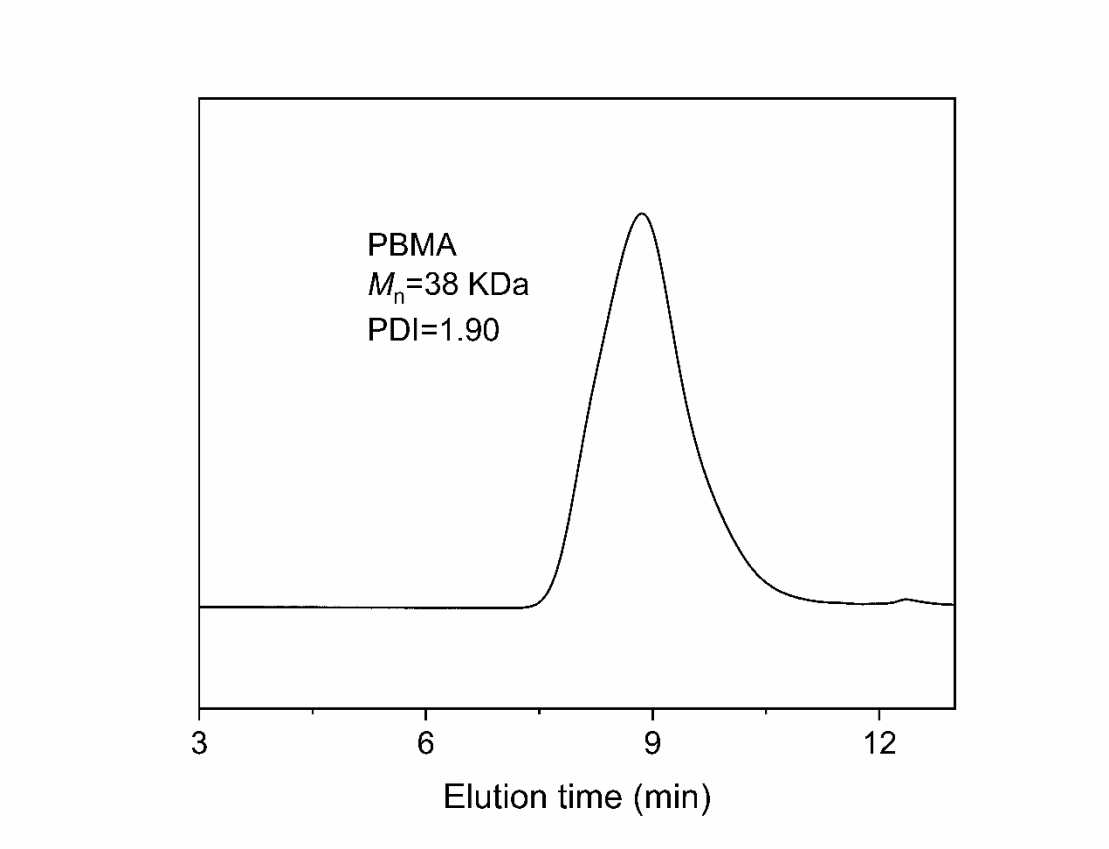

Figure S5. GPC elution curve of the PBMA with DMF as the eluent and PMMA as the standard.

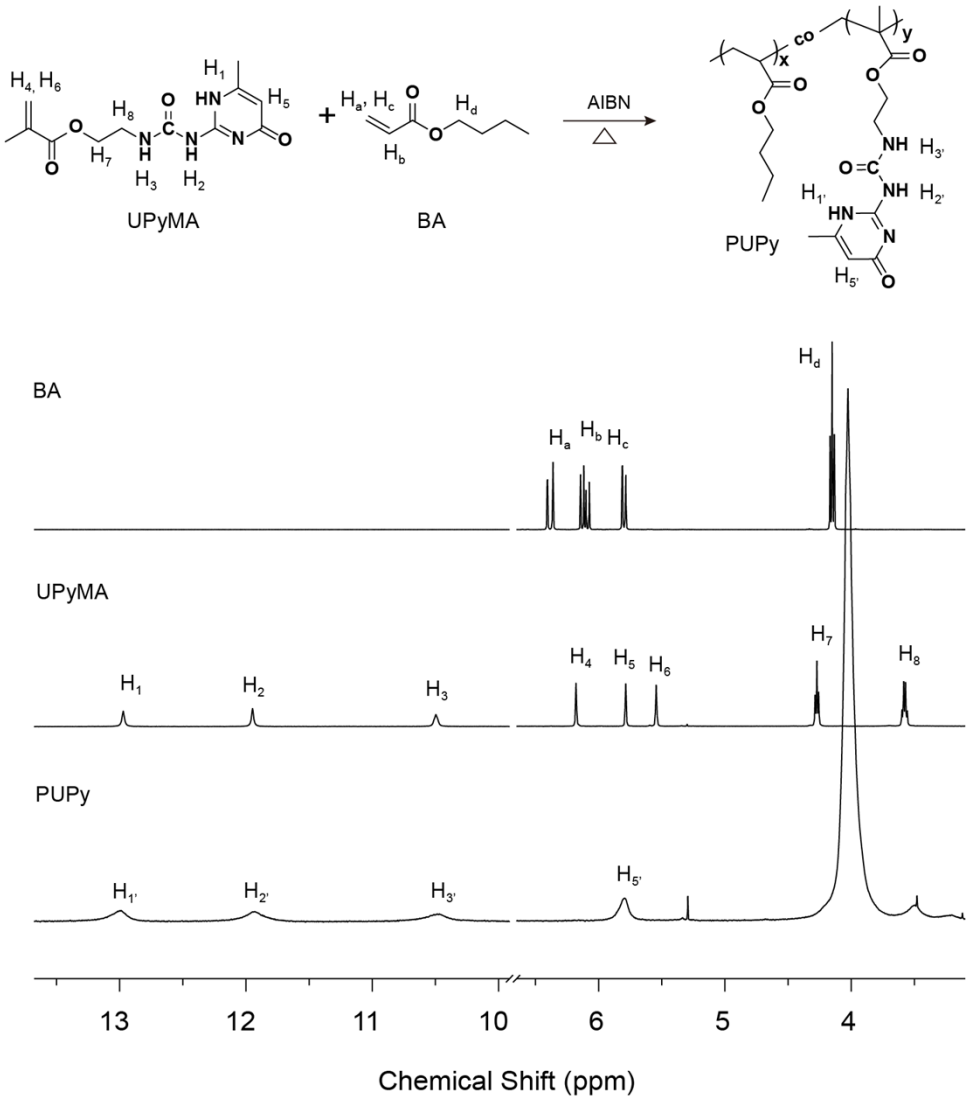

Figure S6. The comparison of partial ^{1}H NMR spectra ($CDCl_3$, 400 MHz, 293 K) of BA, UPyMA, and PUPy.

3. Fabrication of graphene oxide films

Firstly, a GO aqueous dispersion with a concentration of 2 mg/mL was obtained by stirring for 2 h and ultrasonication for 15 min. Subsequently, 10 mL of such dispersion was dropwise added to a vacuum filtration funnel with a hydrophilic filter membrane. After water was filtered out, a piece of GO film was peeled from the filter membrane after a period of natural drying. The GO film (~17 mg) was then immersed in 10 mL DMF containing PUPy, then put it in the oven and heat it at 100 °C for 30min, then adjust it to 70 °C for 2h, and finally place it at room temperature for 3h. The UPy units in the PUPy side chain and the hydroxyl and carboxyl groups of graphene oxide nanoplatelets form hydrogen bond interactions, effectively introducing PUPy into the middle layer of graphene oxide film. Then, the excess PUPy was removed by rinsing with ethanol several times, and the resulting PUPy-bridged graphene oxide film was dried at 50 °C overnight, yielding a PUPy-bridged graphene oxide film, denoted as GUPy (PUPy-bridged oxide graphene) film. By varying the feeding mass of PUPy to 0.2 mg, 2 mg and 20 mg, we prepared different PUPy-bridged graphene oxide films, named GUPy-1, GUPy-2 and GUPy-3, respectively. In the meantime, GPBMA (PBMA-bridged graphene) film was fabricated according to the above processing method by substituting PBMA for PUPy. Besides, GO (graphene oxide) film was also prepared without the incorporation of PUPy and PBMA.

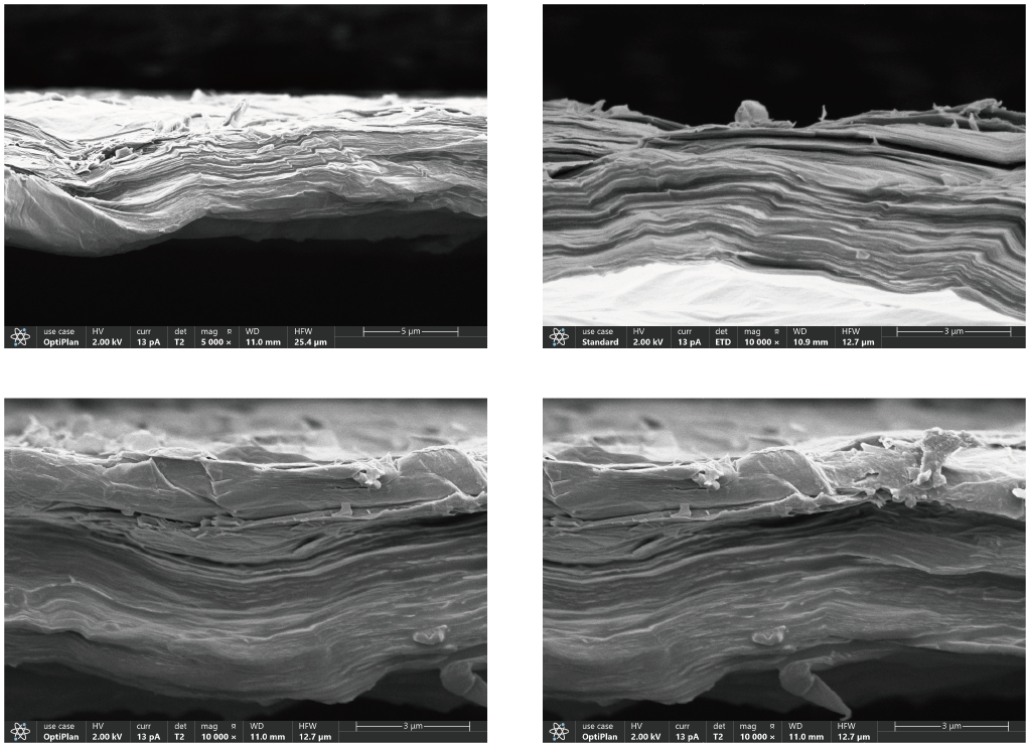

Figure S7. SEM cross-section images of GUPy-2 film.

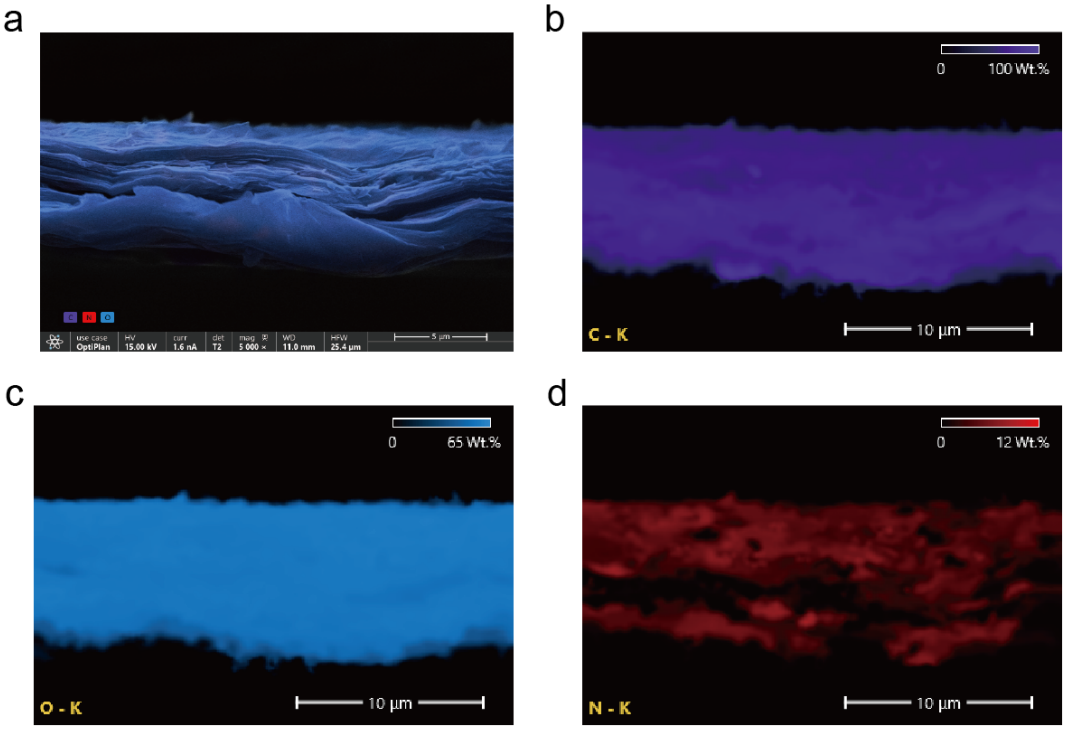

Figure S8. (a) Elemental distribution quant mapping images of GUPy-2 film. Elemental distribution quant mapping images of C (b), O (c), and N (d) corresponding to the film structure in (a).

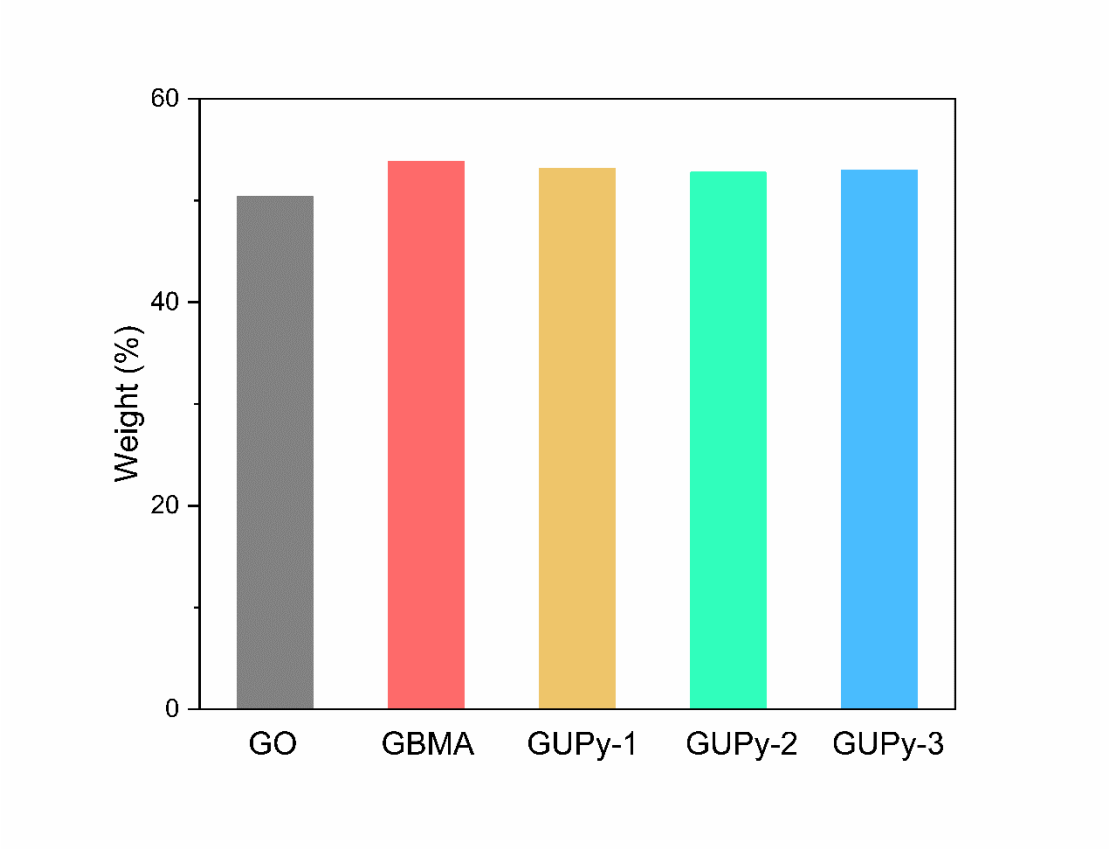

Figure S9. The corresponding thermogravimetric values of GUPy-1, -2, -3, GBMA, and GO films at 450 ℃ from TGA curves.

Table S1. I_D, I_G, and I_D/ I_G values of GUPy-2, GBMA, and GO from Raman spectra.

	I_D	I_G	I_D/ I_G
GUPy-2	615.681	459.257	1.341
GBMA	304.807	237.955	1.281
GO	284.134	22.745	1.276

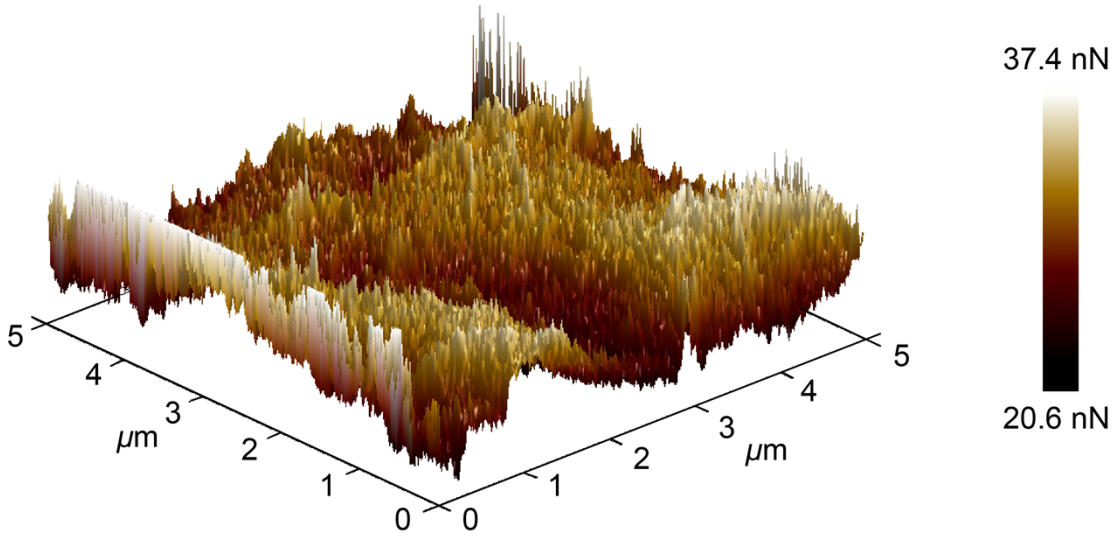

Figure S10. 3D adhesion profile image of GBMA obtained from AFM.

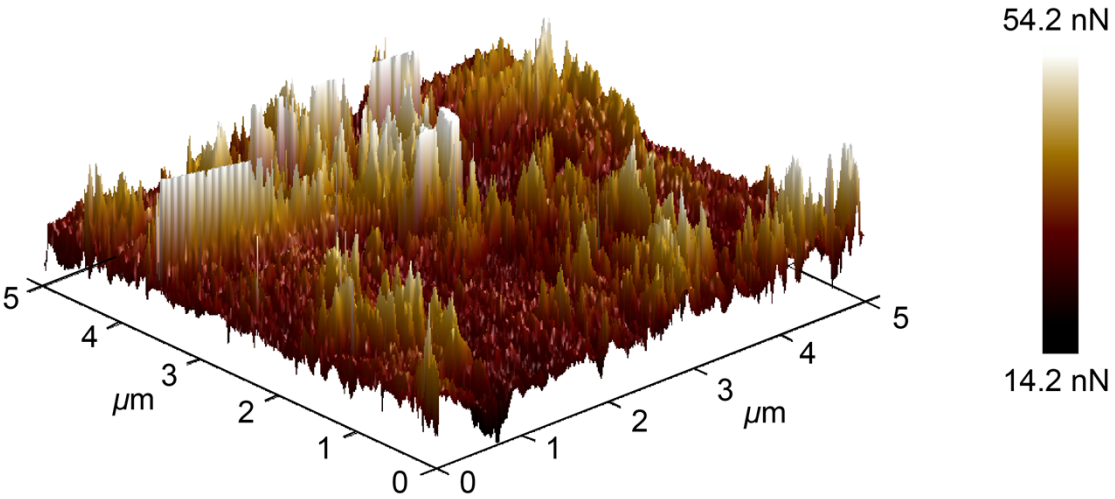

Figure S11. 3D adhesion profile image of GO obtained from AFM.

Table S2. Toughness of GUPy-2, GBMA, and GO calculated based on their stress-strain curves.

	GUPy-2	GBMA	GO
Toughness (MJ/m^3)	19.5	2.3	1.6

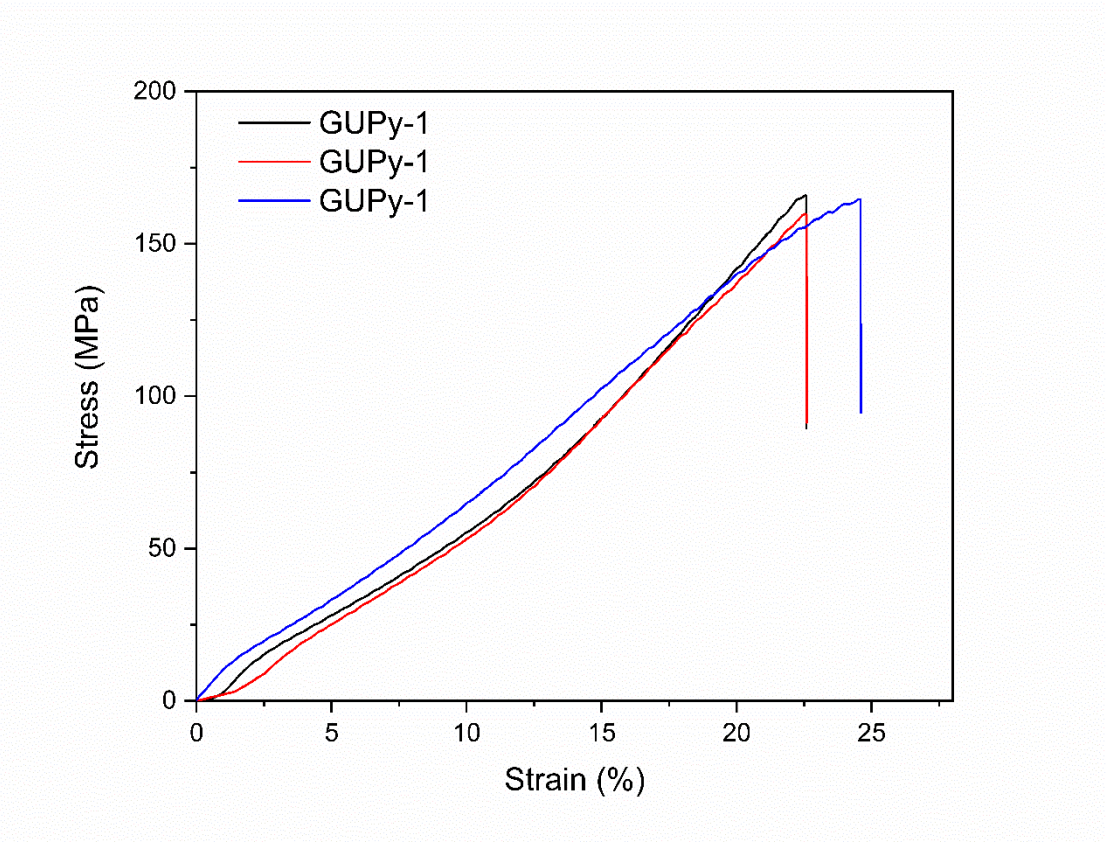

Figure S12. The reproducible stress–strain curves of GUPy-1 films recorded with a deformation rate of 1 mm/min.

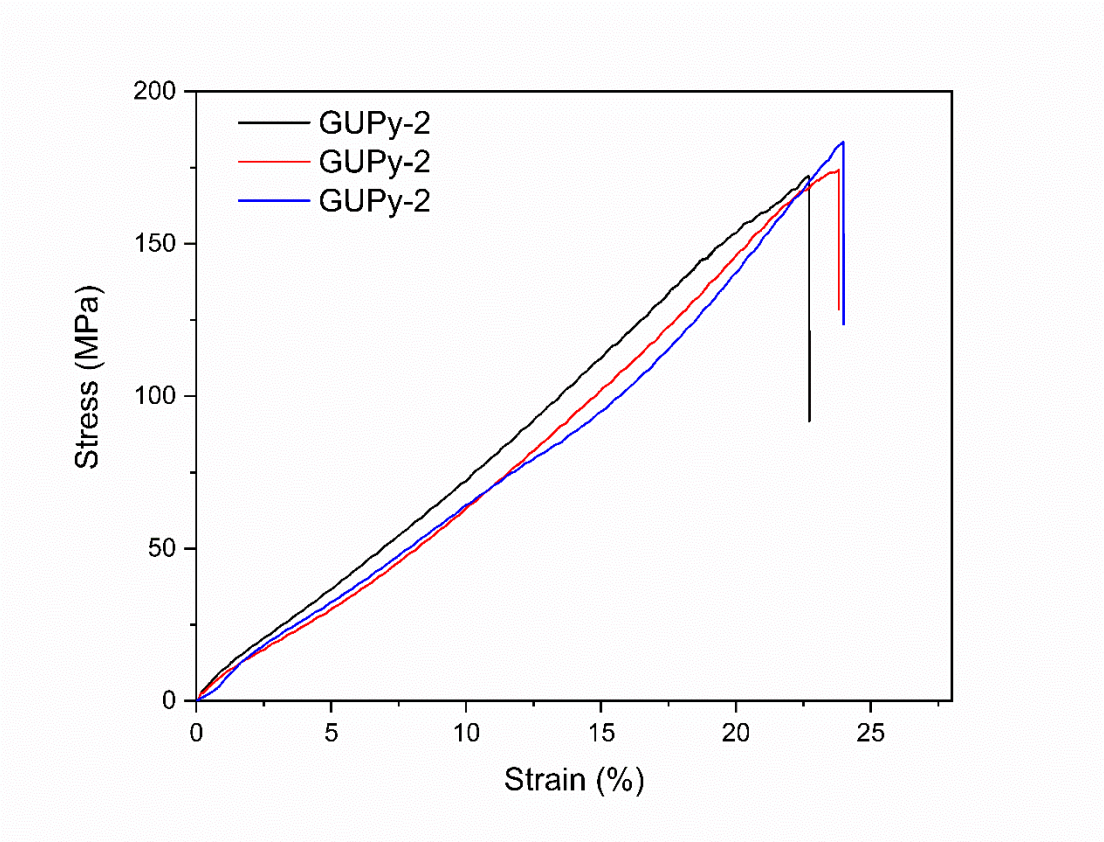

Figure S13. The reproducible stress–strain curves of GUPy-2 films recorded with a deformation rate of 1 mm/min.

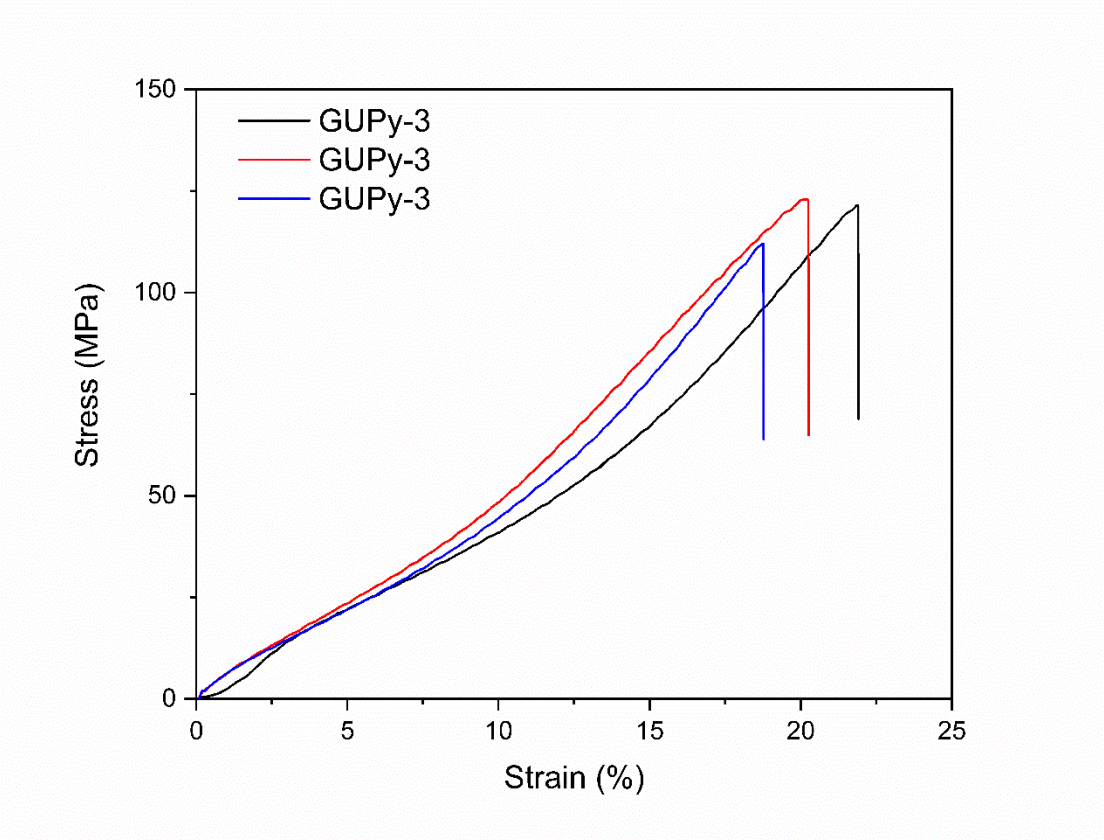

Figure S14. The reproducible stress–strain curves of GUPy-3 films recorded with a deformation rate of 1 mm/min.

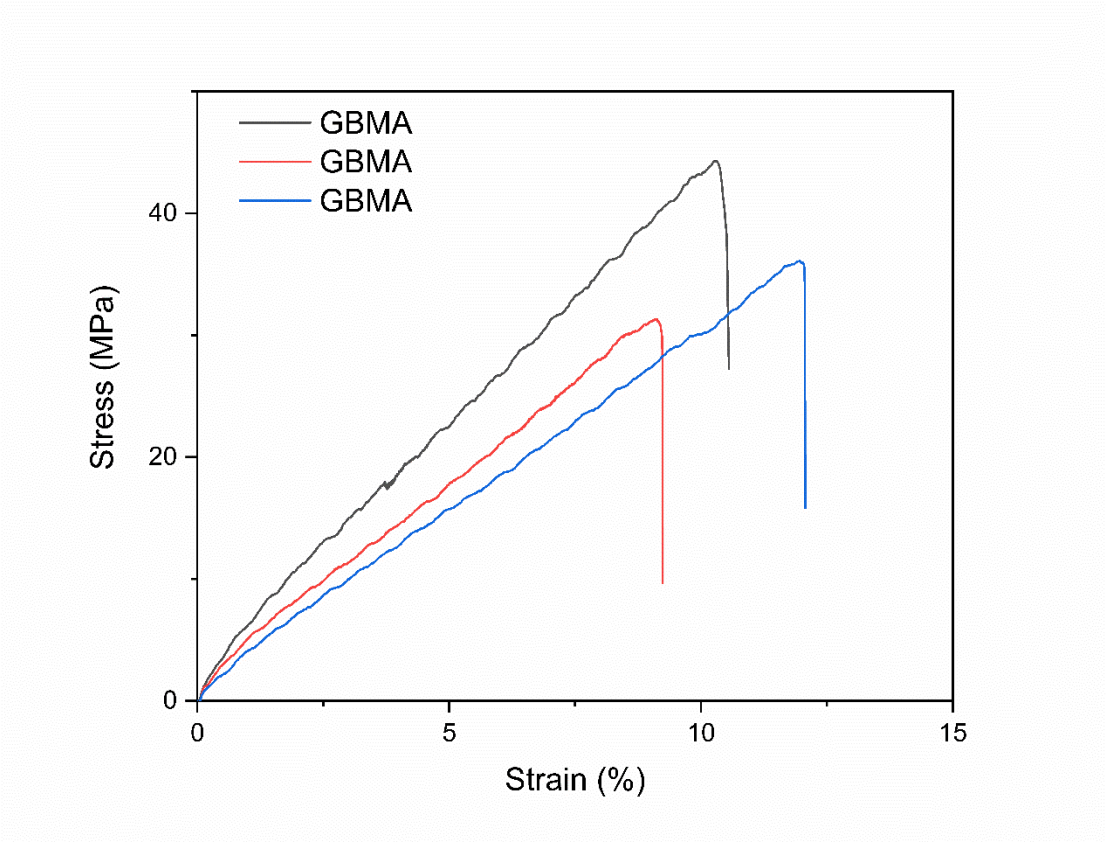

Figure S15. The reproducible stress–strain curves of GBMA films recorded with a deformation rate of 1 mm/min.

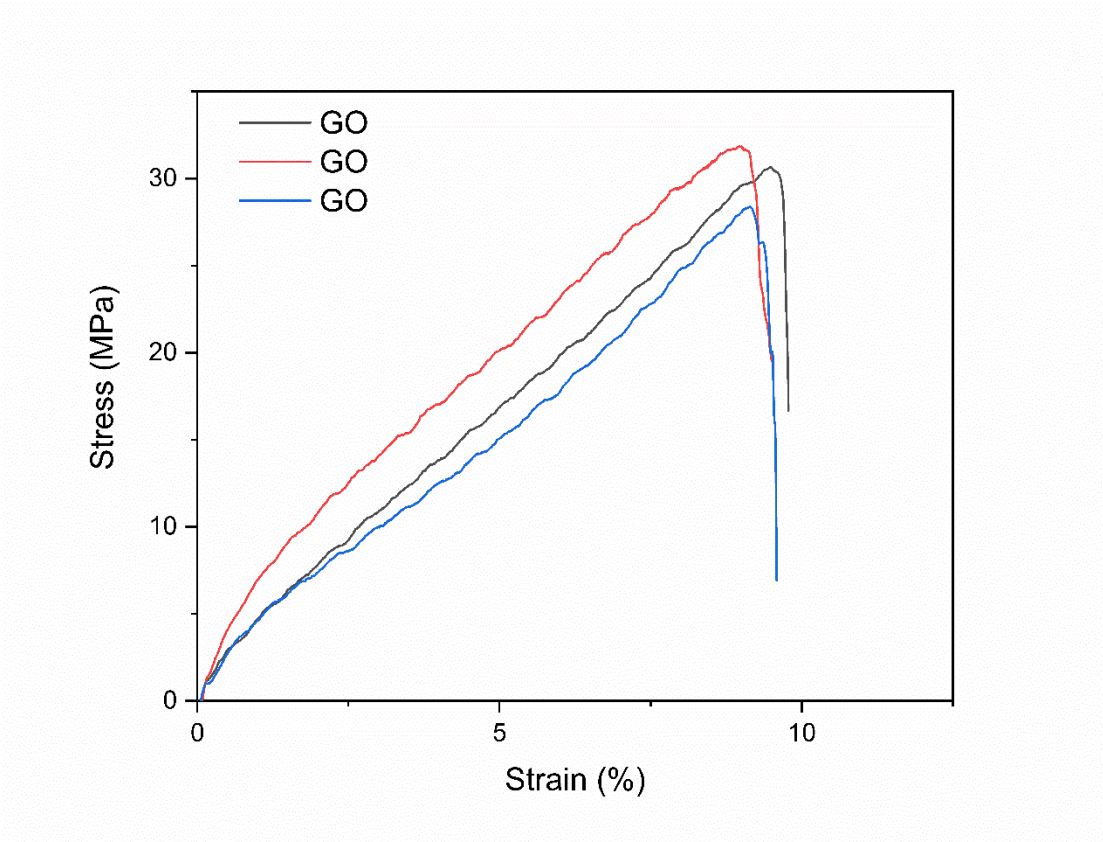

Figure S16. The reproducible stress–strain curves of GO films recorded with a deformation rate of 1 mm/min.

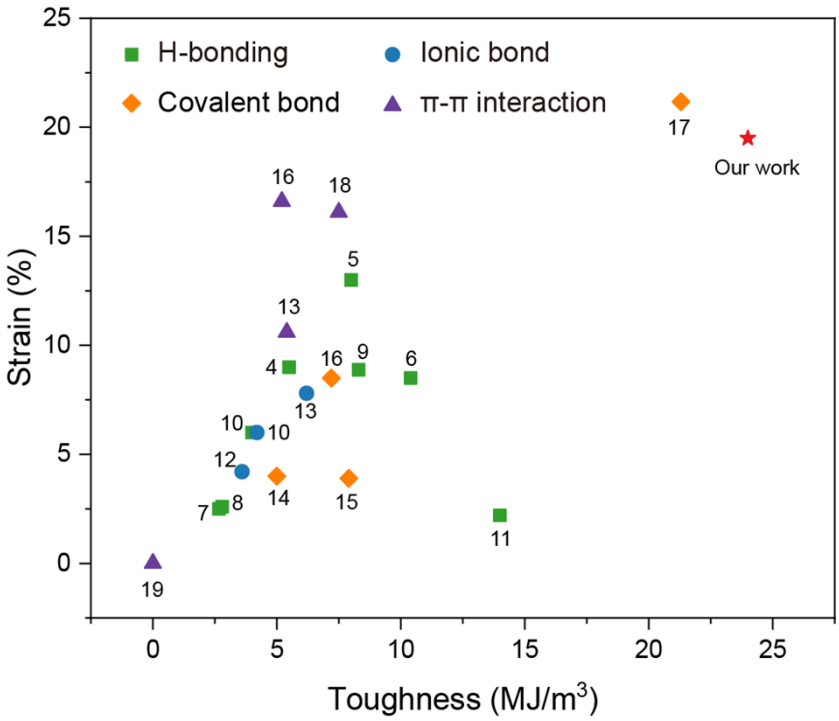

Figure S17. Fracture strain and toughness of previously reported graphene films bridged through different bonding types, including H-bonding, ionic bond, covalent bond, π-π interaction, the GUPy films produced in this study (the numbers in the figure correspond to the serial number of the reference).

References

1. K. Yamauchi, J. R. Lizotte and T. E. Long, Thermoreversible poly(alkyl acrylates) consisting of self-complementary multiple hydrogen bonding, *Macromolecules*, 2003, **36**, 1083−1088.
2. B. Zhou, D. He, J. Hu, Y. Ye, H. Peng, X. Zhou, X. Xie and Z. Xue, A flexible, self-healing and highly stretchable polymer electrolyte via quadruple hydrogen bonding for lithium-ion batteries, *J. Mater. Chem. A*, 2018, **6**, 11725−11733.
3. M. Li, S. Dai, X. Dong, Y. Jiang, J. Ge, Y. Xu, N. Yuan and J. Ding, High-strength, large-deformation, dual cross-linking network liquid crystal elastomers based on quadruple hydrogen bonds, *Langmuir*, 2022, **38**, 1560−1566.
4. Z. Tan, M. Zhang, C. Li, S. Yu, G. Shi, A general route to robust nacre-like graphene oxide films, *ACS Appl. Mater. Interfaces*, 2015, **7**, 15010−15016.
5. Y. Wang, H. Yuan, P. Ma, H. Bai, M. Chen, W. Dong, Y. Xie, Y. S. Deshmukh, Superior performance of artificial nacre based on graphene oxide nanosheets, *ACS Appl. Mater. Interfaces*, 2017, **9**, 4215−4222.
6. N. Zhao, M. Yang, Q. Zhao, W. Gao, T. Xie, H. Bai, Superstretchable nacre-mimetic graphene/poly(vinyl alcohol) composite film based on interfacial architectural engineering, *ACS Nano*, 2017, **11**, 4777−4784.
7. Y.-Q. Li, T. Yu, T.-Y. Yang, L.-X. Zheng, K. Liao, Bio-inspired nacre-like composite films based on graphene with superior mechanical, electrical, and biocompatible properties, *Adv. Mater.*, 2012, **24**, 3426−3431.
8. K. Hu, L. S. Tolentino, D. D. Kulkarni, C. Ye, S. Kumar, V. V. Tsukruk, Written-in conductive patterns on robust graphene oxide biopaper by electrochemical microstamping, *Angew. Chem. Int. Ed.*, 2013, **52**, 13784−13788.
9. S. Wan, H. Hu, J. Peng, Y. Li, Y. Fan, L. Jiang, Q. Cheng, Nacre-inspired integrated strong and tough reduced graphene oxide–poly(acrylic acid) nanocomposites, *Nanoscale*, 2016, **8**, 5649−5656.
10. Q. Zhang, S. Wan, L. Jiang, Q. Cheng, Bioinspired robust nanocomposites of cooper ions and hydroxypropyl cellulose synergistic toughening graphene oxide, *Sci. China Technol. Sc.*, 2016, **60**, 758−764.
11. C.-F. Cao, B. Yu, Z.-Y. Chen, Y.-X. Qu, Y.-T. Li, Y.-Q. Shi, Z.-W. Ma, F.-N. Sun, Q.-H. Pan, L.-C. Tang, P. Song, H. Wang, Fire intumescent, high-temperature resistant, mechanically flexible graphene oxide network for exceptional fire shielding and ultra-fast fire warning, *Nano-Micro Lett.*, 2022, **14**, 92.
12. S. Gong, L. Jiang, Q. Cheng, Robust bioinspired graphene-based nanocomposites via synergistic toughening of zinc ions and covalent bonding, *J. Mater. Chem. A*, 2016, **4**, 17073−17079.
13. S. Wan, S. Fang, L. Jiang, Q. Cheng, R. H. Baughman, Strong, conductive, foldable graphene sheets by sequential ionic and π bridging, *Adv. Mater.*, 2018, **30**, 1802733.
14. W. Cui, M. Li, J. Liu, B. Wang, C. Zhang, L. Jiang, Q. Cheng, A strong integrated strength and toughness artificial nacre based on dopamine cross-linked graphene oxide, *ACS Nano*, 2014, **8**, 9511−9517.
15. Q. Cheng, M. Wu, M. Li, L. Jiang, Z. Tang, Ultratough artificial nacre based on conjugated cross-linked graphene oxide, *Angew. Chem. Int. Ed.*, 2013, **52**, 3750−3755.
16. S. Wan, Y. Li, J. Mu, A. E. Aliev, S. Fang, N. A. Kotov, L. Jiang, Q. Cheng, R. H. Baughman,

Sequentially bridged graphene sheets with high strength, toughness, and electrical conductivity, *Proc. Natl. Acad. Sci. USA*, 2018, **115**, 5359–5364.

17. C. Wang, B. Gao, F. Fang, W. Qi, G. Yan, J. Zhao, W. Wang, R. Bai, Z. Zhang, Z. Zhang, W. Zhang, X. Yan, A stretchable and tough graphene film enabled by mechanical bond, *Angew. Chem. Int. Ed.*, 2024, **63**, e202404481.
18. H. Ni, F. Xu, A. P. Tomsia, E. Saiz, L. Jiang, Q. Cheng, Robust bioinspired graphene film via π–π cross-linking, *ACS Appl. Mater. Interfaces*, 2017, **9**, 24987–24992.
19. Y. Xu, H. Bai, G. Lu, C. Li, G. Shi, Flexible graphene films via the filtration of water-soluble noncovalent functionalized graphene sheets, *J. Am. Chem. Soc.*, 2008, **130**, 5856–5857.